

DEFINING COMPOSITIONAL AND TEXTURAL VARIATIONS IN IRON ORES OF CAPANEMA MINE-MG-BRAZIL USING A JOINT INTERPRETATION OF CORE SAMPLES AND GEOPHYSICAL WELL LOGS

Abel Carrasquilla^{1*} and Luciano Fonseca²

¹Universidade Estadual do Norte Fluminense Darcy Ribeiro, Laboratory of Engineering and Exploration of Petroleum (LENEP), Imboacica, Macaé, RJ, Brazil

²Vale S/A, Mina de Águas Claras (MAC), São Sebastiao das Águas Claras, Nova Lima, MG, Brazil

*Corresponding author: abel@lenep.uenf.br

ABSTRACT. Because density is a fundamental physical characteristic in mineral exploitation, the Brazilian mining company Vale S/A constructed a test site to gather more precise data with the geophysical well log of density. Understanding the lithological units of three drilling holes at the Capanema-Minas Gerais-Brazil Mine better was the primary goal of this calibration. In the study, geological contacts were compared between those determined by caliper, temperature, natural gamma ray, density, neutron porosity, and sonic wireline logs and those identified by descriptions of core samples. The primary goal of the research was to determine compositional and textural variations in iron formations that were brought on by changes in the rock's moisture and hardness. The methodology has shown satisfactory results in detecting the presence of clay and hydrated bodies and the transition between friable and compact itabirites. The possibility of altering exploratory drilling meshes with partial replacement of core sampling by rotary percussive boreholes was thus revealed by these results. With this substitution, mineral exploration would be faster and less expensive while always using well logs to support subsurface geological interpretation.

Keywords: borehole logging, rock samples, iron minerals, compositional variations, textural changes.

INTRODUCTION

Regional geological mapping, aerial geophysical surveys, and subsurface research are part of the industry's mineral prospecting process (Kearey et al., 2002). According to this viewpoint, conventional subsurface exploration through drilling wells yields geological medium's core samples (CS). Although it offers detailed, localized information, this method is costly and time-consuming (Oliveira et al., 2011; Darling, 2005). Even though they employ indirect measurements, the geophysical well logs (GWL) are helpful (Schön, 2011). Nevertheless, combining the two methodologies can result in more accurate data while taking less time and spending less money (Rider,

2002; Luthi, 2001). GWL offers several advantages to assist drilling data in defining geological contacts, determining depths, and conducting correlations between wells. However, to complete a job like this, GWL must be adjusted for the effects of drilling mud, mud-cake, invasion, well roughness, etc. (Rashidi et al., 2009; Cannon, 2016).

The study area for this project was Capanema Mine, located in the Iron Quadrangle's central location in Minas Gerais State, Brazil (Figure 1). Itabira Group lithologies, represented by itabirite and hematite rocks of the Caue Formation (Franco, 2003), are where the mineralization in this mine takes place. The poor thick layer of ore (PLO) that covers these lithologies is known as the Itabira Group (Guimaraes et al., 1986). According to Vaz de Melo and Seabra (2000), the structural geology of the area is quite intricate, having been folded by numerous generations of deformational events that duplicated the layers and altered their apparent thickness.

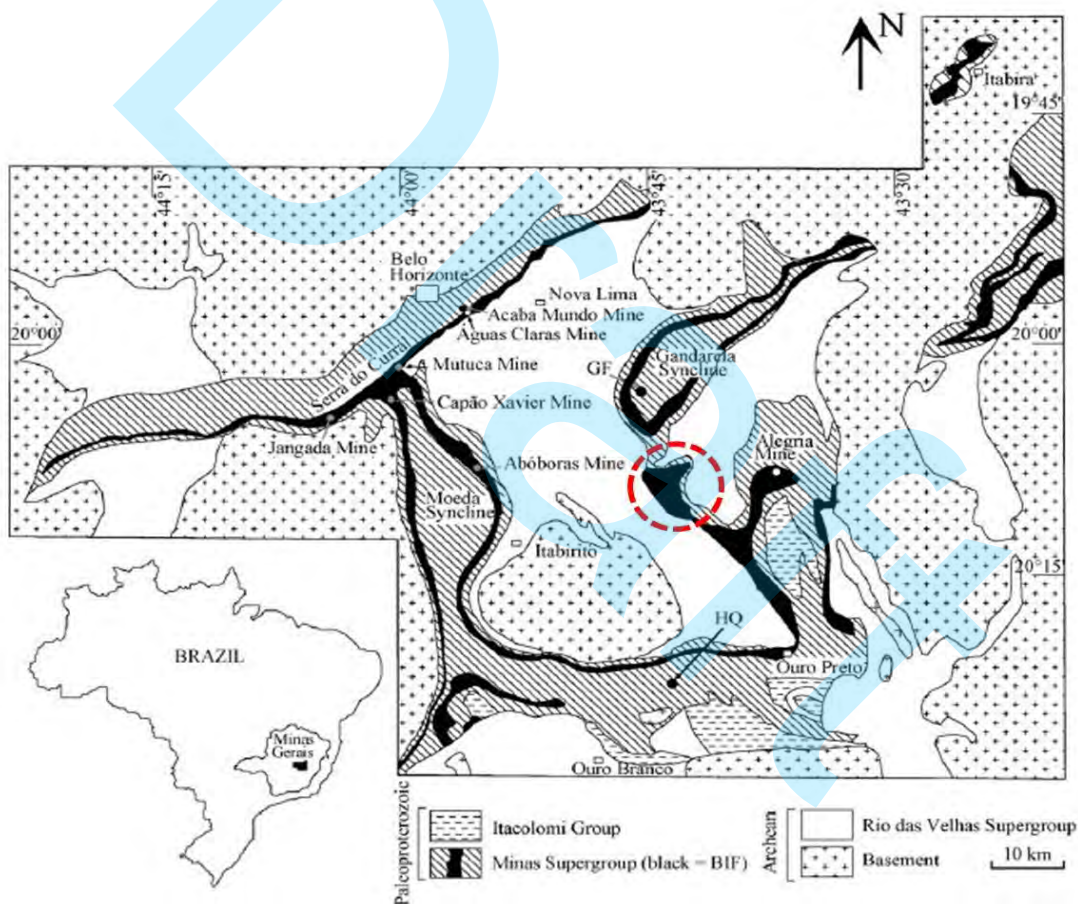


Figure 1. The geographical location of Iron Quadrangle in Minas Gerais State, highlighting the regional geological outline and Capanema Mine (dashed red circle). The iron formation units are black, making up the mountains that define the structure: Curral at the north, Moeda, Itabirite at the west, Ouro Preto at the south, and Itabira at the east. The other symbols show more lithological units (Spier et al., 2007).

To shorten research time and save expenses, the overall goal of this effort was to enhance iron ore exploration through the integration of CS and GWL data. It specifically aimed to find clay horizons, hydrated bodies, the boundary between friable and solid itabirites, the thickness of the weathering layer, and strata that were most abundant in iron (Fe).

MATERIALS AND METHODS

The Brazilian Mineral Company Vale constructed a test site in a controlled environment (Figure 2) to confidently determine this petrophysical property of the geological formations due to the need for accurate measurements of density log in the ore industry and as part of this study (IPT, 2011). Capanema Mine demonstrated key characteristics to develop this work by showcasing features that allow for a systematic and controlled study (Figure 3).

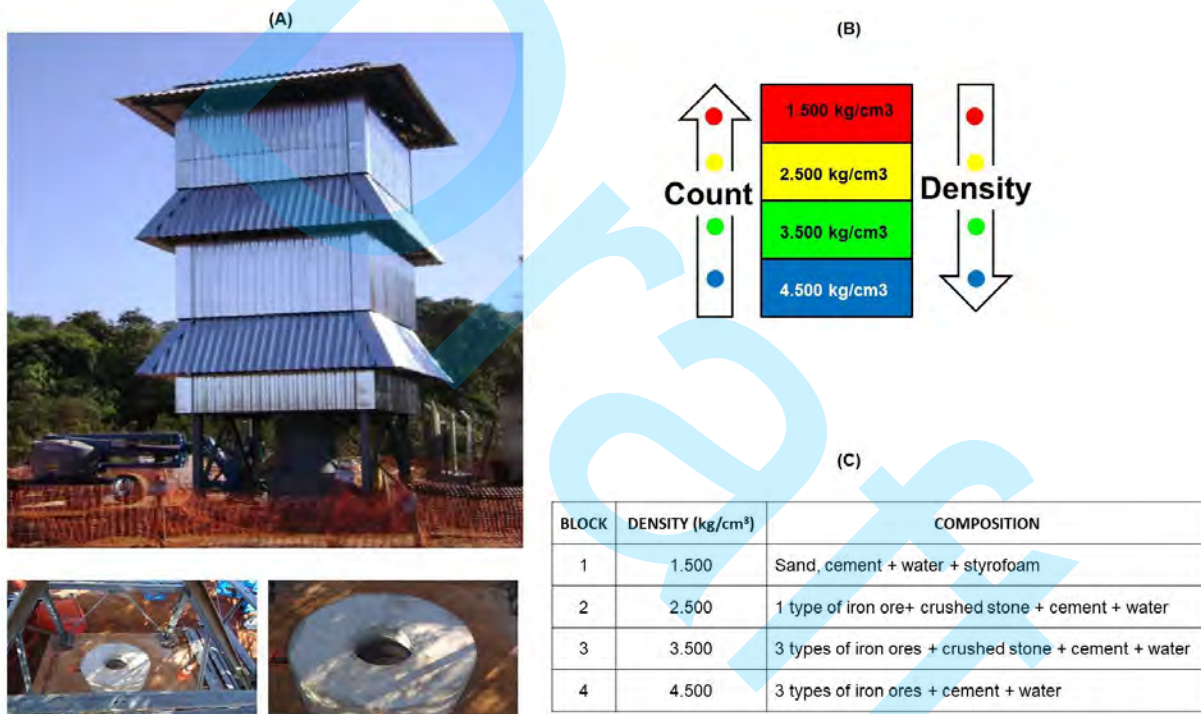


Figure 2. A) Tower in the test site to measure density log. B) Block positioning into the tower with a central hole where GWL tools descend. C) Provision of the blocks with respective density, composition, and counting (IPT, 2011).



Figure 3. Location of boreholes FD28, FD29, and FD31 in Capanema Mine. Dashed lines in blue indicate the position of the geological sections (Fonseca, 2014).

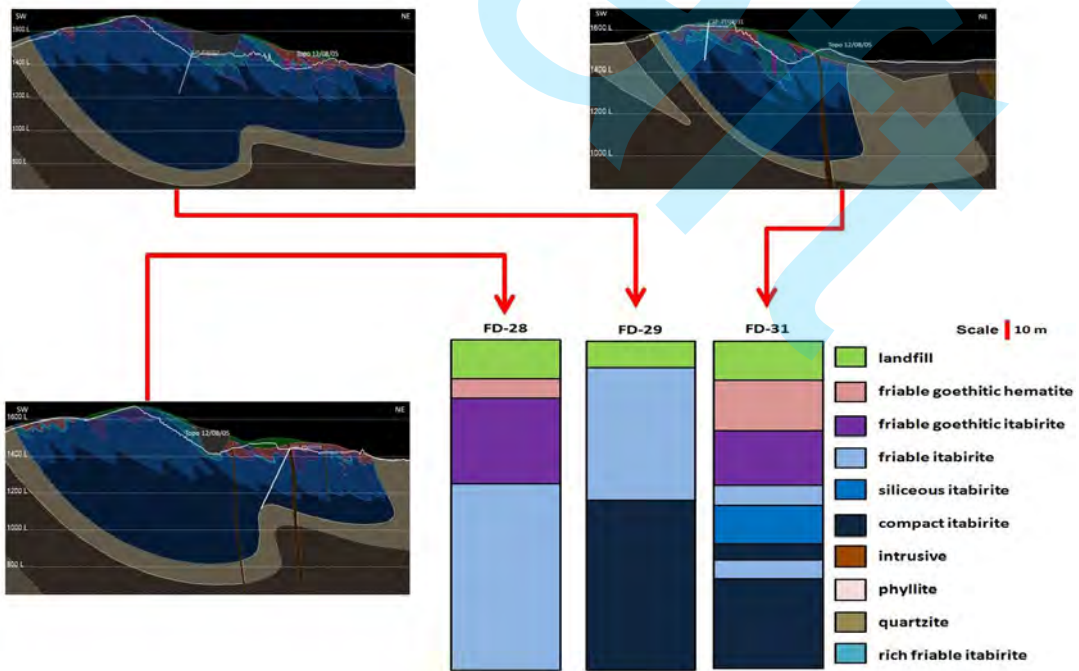


Figure 4. Interpreted geological sections for boreholes FD-28, FD-29, and FD-31. The position of each borehole is highlighted in white in the section (Fonseca, 2014).

The geological sections of Capanema Mine are based on the interpretation and chemical analysis of samples from boreholes FD-28, FD-29, and FD-31. This extensive database of the mine aids in understanding the regional context (Figure 4). With this knowledge, data were integrated to evaluate significant GWL changes in response to CS compositional and textural changes. The caliper (CAL), temperature (TEMP), natural gamma ray (GR), density (RHOB), neutron porosity (NPHI), and sonic velocity (Vp) wireline logs were utilized in the study. It is crucial to make it clear that the NPHI log has "pu" (porosity units) or "snu" (signal neutral units) units in the figures presented in the article. The highest counts in the variation of the NPHI log in the "snu" unit denote lower hydrogen concentrations and, as a result, lower porosities. The variation in the mineralogical composition may be exhibiting intervals with a higher percentage of hydrated minerals or the presence of water in the rock's porosity may be reflected in this. The logs were collected by Weatherford Company in open holes of this mine (Pena, 2013). Subsequently, the softwares WellCad (2014) and Matlab (2014) were used to process, plot, and make the interpretation of the logs.

RESULTS AND DISCUSSIONS

For the three wells, the chemical laboratory analysis of CS reveals Fe percentages of roughly 40% and 60% up to 80.0 m (Figure 5A). On the other hand, the content of silica (SiO_2) increases with a depth of over 30.0% (Figure 5B), and the concentration of alumina (Al_2O_3) decreases to less than 2.0% after 40.0 m in wells FD-28 and FD-31 (Figure 5C). Therefore, all geological sections have a consistent pattern, with higher clay levels at the start of boreholes and lower clay levels below 20.0 m. This material, classified as a modified ferruginous rock from 3.6 to 76.9 meters in depth, is known as weathered hematite in the area. It is a goethite or hydrated hematite with high iron content (60% Fe) (Figure 5A), low SiO_2 (Figure 5B), and elevated levels of contaminants like Al_2O_3 (Figure 5C), phosphorus (Figure 5D), and high values of loss on ignition (PF) because of the abundance of hydrated minerals (Figure 5E) (Fonseca, 2014).

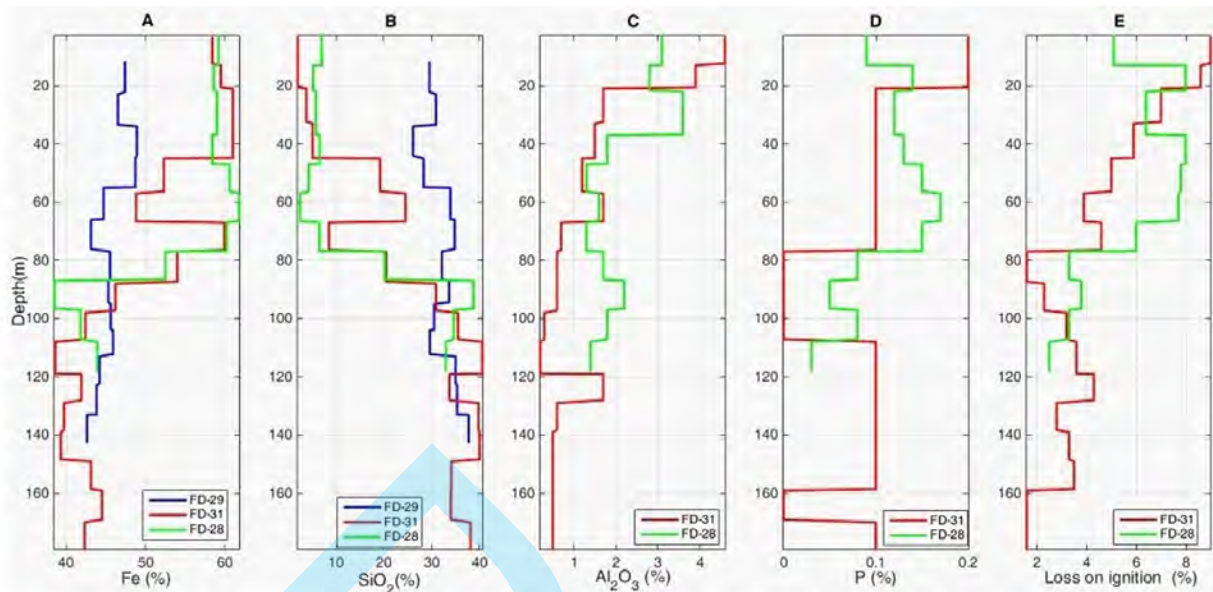


Figure 5. Chemical analysis of samples from wells FD-28, FD-29, and FD-31: (A) Fe, (B) SiO_2 , (C) Al_2O_3 , (D) P, and (E) loss on ignition (Fonseca, 2014).

In each well, the particle size analysis showed a coarser material after 100.0 m deep (Figure 6A), with a thinner material close to the surface (Figures 6B, C, and D). In these figures, the classification of G1 to G4 values indicates the percentage of materials retained in different sieve size classifications, where $G1 > 8.00$ mm, $1.00 < G2 < 8.00$ mm, $0.15 < G3 < 1.00$ mm, and $G4 < 0.15$ mm (Fonseca, 2014). For the well FD-29, Figure 7, prepared from Figure 6A, shows a linear increase of particle size with depth described for the equation $G1 = 1.3 \times \text{Depth} - 8.7$, different from the linear relationship $G1 = \text{Depth}$, also shown in this figure. Moreover, this figure also shows, respectively, green, yellow, and blue circles for three physical horizons of this well classified as friable (IF), semi-compact (IS), and compact (IC) itabirites. The grouping analysis k-means, which aims to partition n observations into k clusters, drew these circles, wherein each observation belongs to the aggregate with the nearest mean (Matlab, 2014).

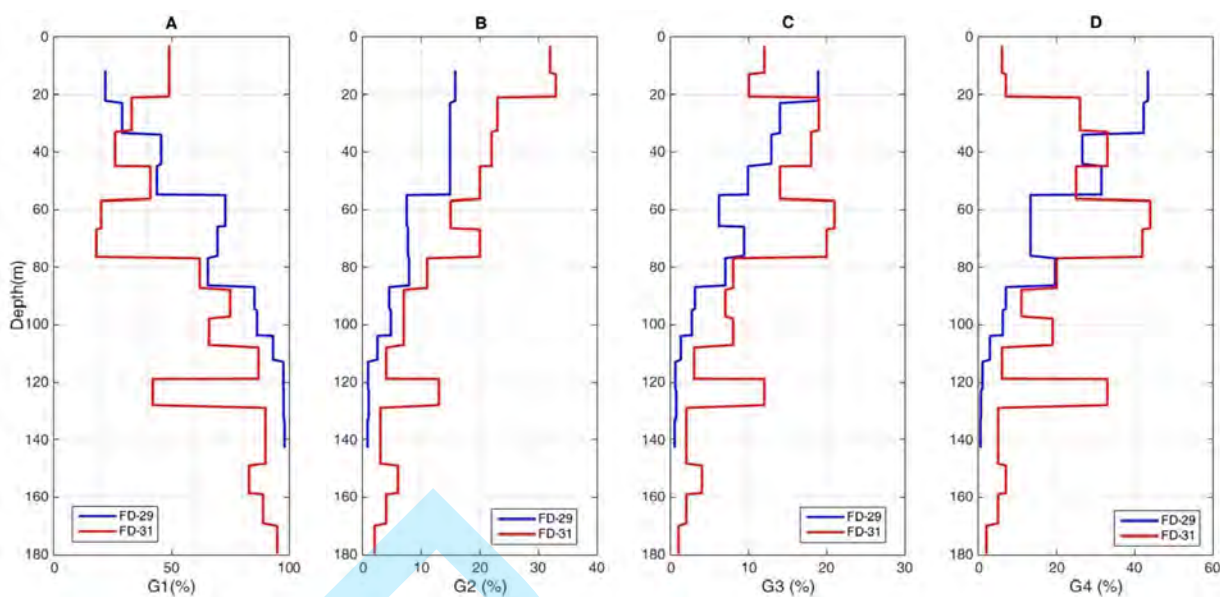


Figure 6. Particle size analysis in wells FD-29 and FD-31 with (A) $G1 > 8.00$ mm; (B) $1.00 < G2 < 8.00$ mm; (C) $0.15 < G3 < 1.00$ mm and (D) $G4 < 0.15$ mm (Fonseca, 2014).

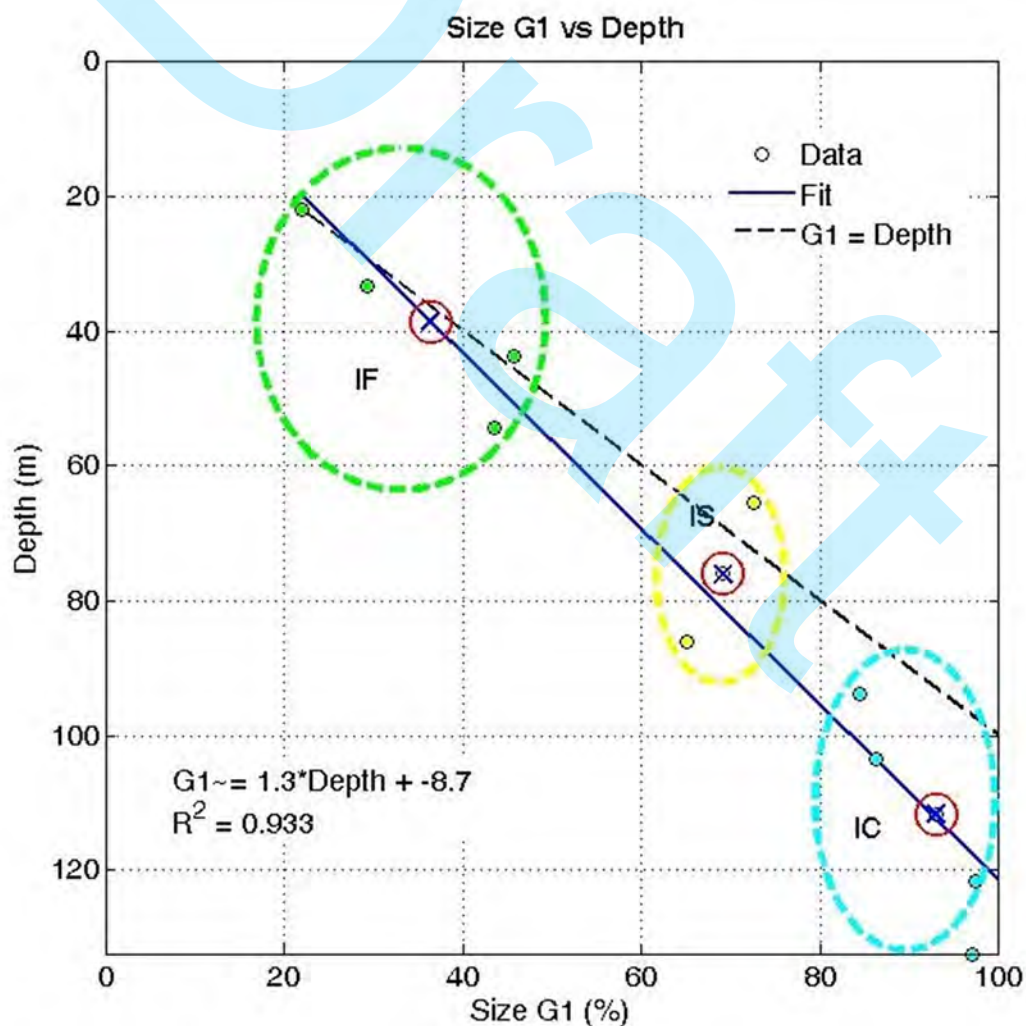


Figure 7. Graph of particle size of the dispersion curve of thick interval (G1) in borehole FD-29 versus depth, indicating increased compaction with depth and showing the

subdivision in groups of friable (IF), semi-compact (IS) and compact (IC) itabirites (Fonseca, 2014).

Borehole FD-28 reached a maximum depth of 360.0 m, whose geological description shows a shallow landfill of 20.0 m, passing for goethite hematite up to 21.0 m, followed by an ocher sericite phyllite up to 37.0 and a friable goethite itabirite up to 77.0 m. From there, it goes to the end of the borehole composed of friable itabirites with diverse levels of compactness and progressively lower levels of iron (Figure 4). The logs GR, RHOB, TEMP, and CAL recorded the first 98.0 m of this borehole (Figure 8 shows only the first 40.0 m). GR log shows low range values that indicate a reduction in the presence of clay to 27.0 m, wherein the material increases up to 33.0 m (dashed red rectangle in Figure 8). In Figure 9, at a depth of 51.0 m, the average value of the measured RHOB changes from 3.0 g/cm³ to 3.5 and 4.0 g/cm³, which can be explained by increased iron content between 47.0 and 77.0 m, particularly in the range from 56.3 m, which assumes a peak concentration (red arrow in Figure 9, which only shows the depth between 48 to 56 m). CAL log also shows a reduction in borehole diameter after 51.0 m, showing a transition to a more consistent material (blue arrow in Figure 9, which only shows the depth between 48 to 56 m). However, from 77.0 m, a considerable reduction in the contents of Fe is noticed without declines in RHOB values, decreasing the porosity caused by increased compression (not shown in this work). Although it is noticeable in chemical analysis and geological description, the transition from weathered material to siliceous itabirite is not evident in the logs. GR log suggests the presence of clays in itabirites throughout the logged interval, supported by the results of the chemical analysis with alumina results above 1.5% up to 107.0 m depth, which is the main kaolinite clay mineral.

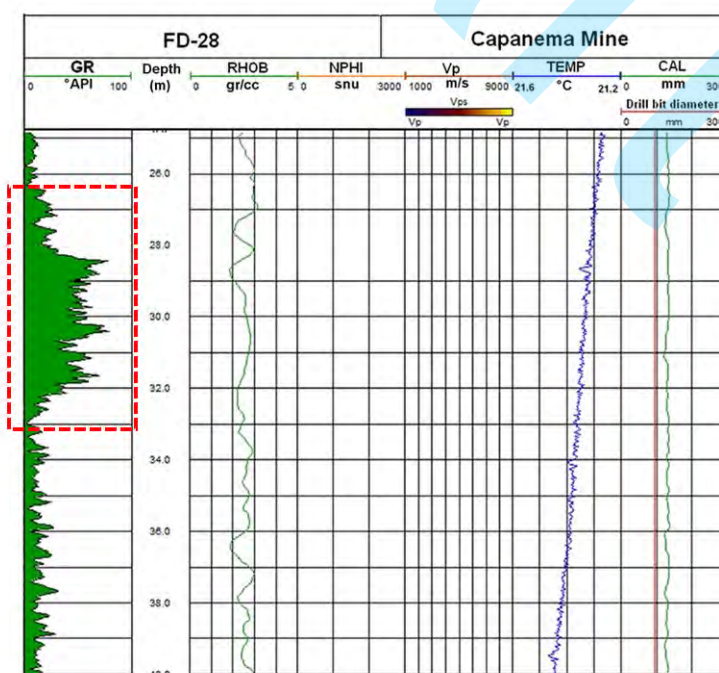


Figure 8. GR log registering the mafic intrusive in depth between 27.0 to 33.0 m in borehole FD-28. The RHOB, TEMP, and CAL logs are also shown on subsequent tracks (Fonseca, 2014).

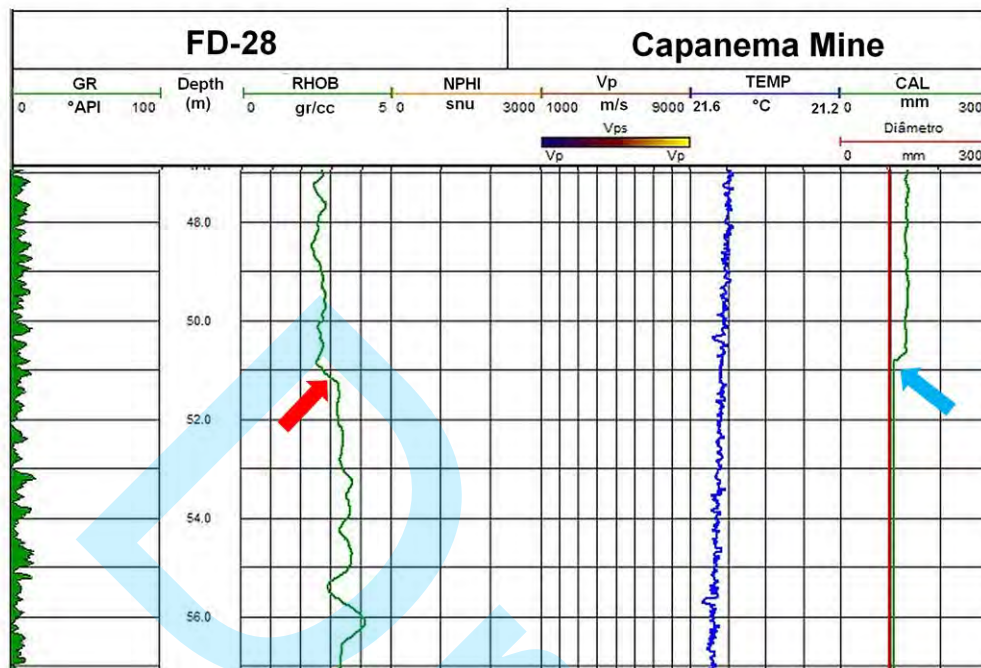
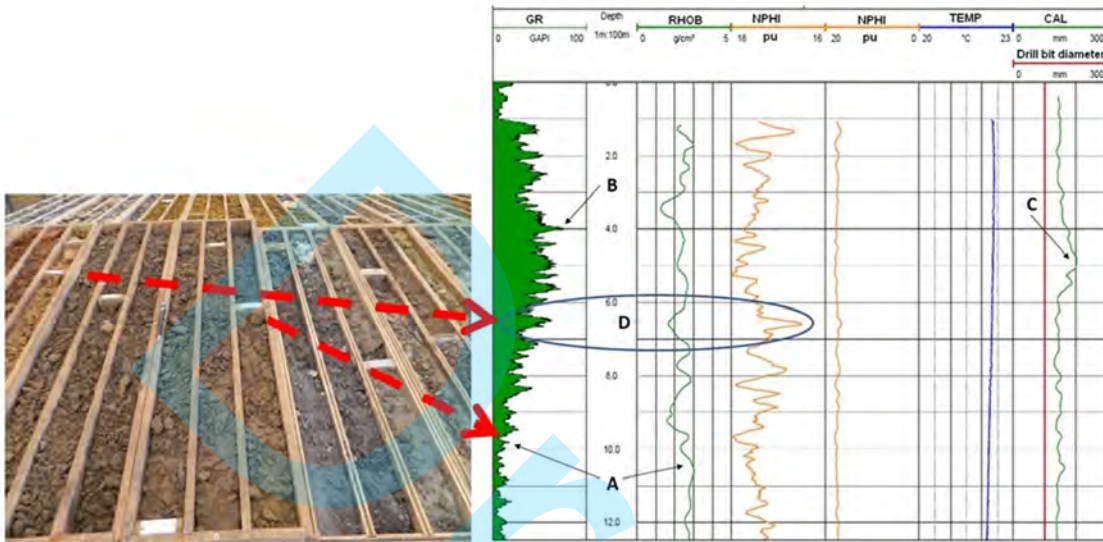


Figure 9. Log details in FD-28 borehole. GR, RHOB, NPHI, Vp, TEMP, and CAL logs from left to right. Arrows show changes in RHOB (red) and CAL (blue) logs at 51.0 m (Fonseca, 2014).

Borehole FD-29 reached a depth of 252.9 m, whose geological description indicated a landfill until 12.0 m, getting a friable itabirite after this and evolving to a compact itabirite at 60.0 m (Figure 4). Throughout the hole, itabirites proved slightly hydrated with variations in particle size and compactness, ranging from a brittle compact with clay intercalations (left side of Figure 10). It is possible to see a difference of around 4.0 m between the core sample and log because the range of approximately 6.0 m describes a sericite phyllite zone, representing an altered mafic rock intrusion. The measurement of the GR, RHOB, NPHI, Vp, TEMP, and CAL logs got to 133.0 m in this wellbore. On the right side of Figure 10, the GR log shows a sharp drop in the shaliness around 10.0 m, coincident with the more rectilinear pattern of the RHOB curve, which can reflect the contact between the landfill and itabirite. In B, the GR log shows a shaly peak, which coincides with collapses in the borehole, showing a larger diameter measured by the CAL log in C. In D, the decrease in NPHI coincides with a drop point in the RHOB log and a high concentration of clay at the landfill, as shown by the GR log. On the other hand, the CS of this hole is depicted on the left of Figure 11 at depths ranging from 19.0 to 28.30 m, displaying an increase in compression in itabirite ore at a depth of 26.0 m, making the CS more cylindrical. Details of the GR log are shown to the right of this figure, followed by the NPHI and RHOB logs. RHOB increased to 26.0 m depth (Figure 11, dashed red arrow and blue circle), and the NPHI log showed a corresponding decline in porosity. Figure

12 displays the final lithological description alongside the details of the GR, RHOB, NPFI, Vp, TEMP, and CAL logs, from left to right. The RHOB log increases, and the NPFI and CAL logs decrease at 63.0 m depth (break 1). A new NPFI fall and increased RHOB logs occurred at 75.0 meters (break 2). The water table changes the RHOB logs around 85.0 m below this, also picked up in the TEMP log, as shown by the inverted delta.



. Details on logs of borehole FD-29: (A) sharp fall in shaliness at 10.0 m, coinciding with the most rectilinear pattern of RHOB log, reflecting the contact landfill-itabirite; (B) peak of shaliness coincident with the collapse in borehole walls registered on CAL log in (C); (D) decrease in porosity recorded in NPFI log, coinciding with a drop in density (RHOB log) and increased concentration of clay in the landfill (GR log) (Fonseca, 2014).

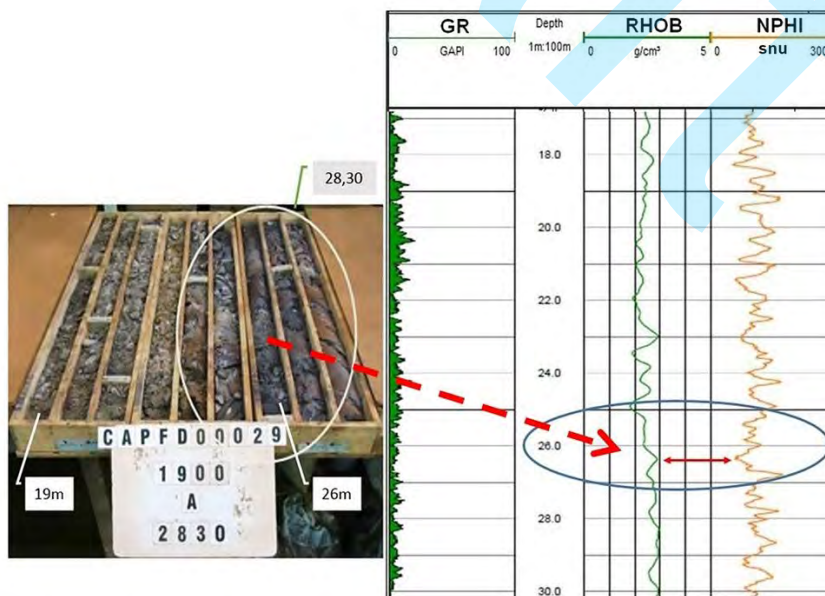


Figure 11. At the left drill core for borehole FD-29 between 19.0 and 28.3 m depth, showing increased compactness of the itabirite ore around 26.0 m, with cores proving

more cylindrical. The right part of the figure shows the GR, RHOB, and NPHI logs, being observed an increase in the density level slightly above 26.0 m depth correlated with a decrease in the NPHI log (Fonseca, 2014).

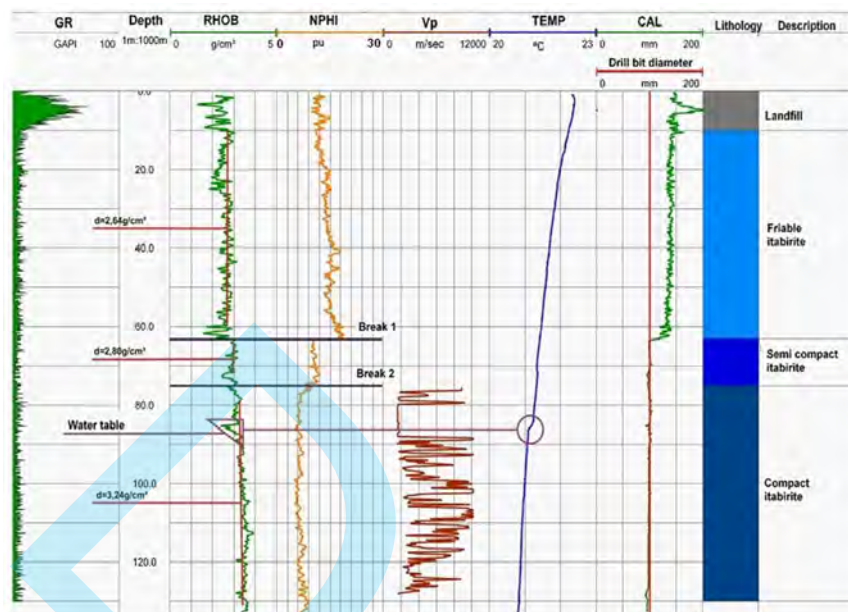


Figure 12. GR, RHOB, NPHI, Vp, TEMP, and CAL, logs of borehole FD-29, together with lithology and its description. From 63.0 m depth, an increase in the RHOB log is recognized, showing reductions in NPHI and CAL logs (break 1). At 75.0 m, there is a new fall in the NPHI log and an increase in the RHOB log (break 2). The inverted delta with little change in the CAL log around 85.0 m was interpreted as the water table, also observed in the TEMP log. Vp shows an increase toward the bottom of the borehole, interpreted as a transition zone of itabirites with different degrees of compactness, friable to 63.0 m, semi-compact, and compact from 70.0 m to the end (Fonseca, 2014).

The Vp log, on the other hand, reaches a low value of 2000.0 m/sec when it reaches 80.0 m, increasing the acoustic waves' transit time. All of this behavior was explained as a zone of itabirites transitioning from friable to semi-compact to compact after 75.0 m (Figure 12), with varying degrees of compression. After 100.0 m, RHOB, NPHI, and Vp log details show an increase in density, a decrease in porosity, an increase in compression, and a subsequent increase in Vp, likely due to a rise in the concentration of iron minerals (Figure 13). As a result, the B level exhibits a transition zone-like pattern of little NPHI growth, decreased RHOB, increased compression, and increasing Vp log. In the presence of hematite horizons with high iron content, for example, the compression/porosity factor was more important than the rock's chemical composition, which differed from the situation in another borehole under study (Fonseca, 2014).

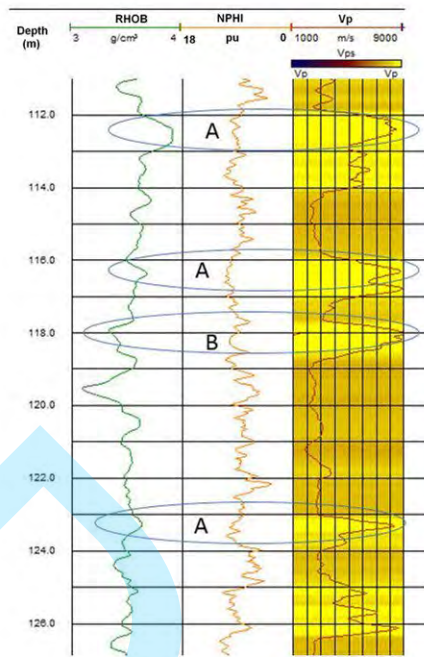


Figure 13. Details of RHOB, NPHI, and Vp logs in borehole FD-29 show (A) increased compactness, reduced porosity, and increased density. B) Increased compactness, reduced porosity, decreased density, and increased Vp, probably because of the increased concentration of iron minerals (Fonseca, 2014).

Only 70.0 m of the logs were measured in the borehole FD-31, but with the existence of CS. It passed through a landfill up to a depth of 12.0 m, and from this point up to a depth of 18.9 m, PLO was discovered with only tone variations (left side of Figure 14). Around 22.3 meters down, a red clayey PLO changed into a sandy yellow goethite hematite. From this point, the composition gradually changed to friable goethite hematite at 45.0 m, then to friable goethite itabirite at 76.5 m, which gradually changed to a compact siliceous itabirite. Since all the sections up to this depth are shallow and weathered, goethite, kaolinite, and gypsum are abundant and typically found in hydrated environments (Figure 4). The laboratory analysis supported this interpretation, which shows high concentrations of Fe, SiO₂, and Al₂O₃ at this depth (Figure 5). A decrease in Fe and an increase in SiO₂ contents, both goethite, can also be used to identify the hematite to itabirite transition (Figure 5). The variations in RHOB and CAL logs up to 12.0 m of well FD-31 show the shallow landfill, interpreted as the change from a sandy to a clayey horizon of PLO (right of Figure 14). The presence of clays due to mineralogical modifications likely causes a decrease in the RHOB log and an increase in CAL logs. Still, there is also a decrease in porosity and an increase in density due to the exit of soluble elements (red arrow in Figure 14), as seen in GR, RHOB, and NPHI logs. PLO, identified as a clay layer with variable porosity and density in the GR, RHOB, and NPHI logs, is designated for the 12.0 to 18.9 meters depth range. Smaller porosities may have altered NPHI logs due to water in the pores or higher concentrations of hydrated minerals. The variations in RHOB, NPHI, and CAL logs indicate a more porous horizon with potential voids in the 18.9 - 22.3 m depth range. The RHOB log does not show a grade from PLO to goethite

hematite below 22.3 m. Nevertheless, the GR log shows a progressive drop in clay concentration.

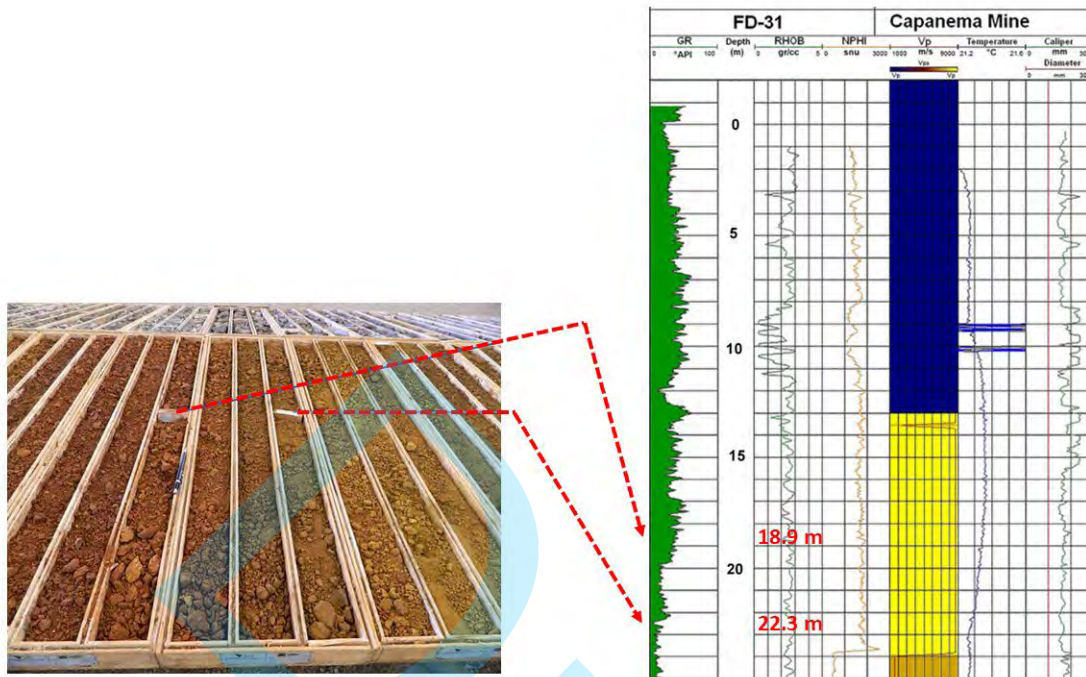


Figure 14. Borehole FD-31: (A) CS showing transitions between landfill to PLO (18.9 m) and PLO to yellow goethite hematite (22.3 m). (B) Well logs from left to right: GR, RHOB, NPHI, Vp, TEMP, and CAL. The red arrow indicates the transition between landfill and PLO, the black arrow indicates the transition between PLO to goethite hematite, and the blue arrow indicates the water table (Fonseca, 2014).

However, the CAL log reveals that the smaller diameters without asperities or breaking points are a more robust material (black arrow in Figure 14). On the other hand, variations in the Vp, NPHI, TEMP, and CAL logs at 24.0 m depth are linked to a change in porosity and are taken to indicate the presence of the water table (blue arrow in Figure 14). After that, the GWL did not exhibit notable changes, moving to clayey levels with improved borehole wall stability. The RHOB log displays a "saw" pattern between 36.0 and 43.0 m, increasing from 2.5 to 2.9 g/cm³ because of an iron-richer interval (not shown). It then provides a drop that may indicate the change to the goethite itabirites described at 45.0 m. According to the geological description, a gray siliceous itabirite abruptly contacts another ochre and clay itabirite at 70.0 m.

The results of this study also point to potential changes in the drilling mesh, including a partial replacement of CS boreholes with rotary-percussive (RP) boreholes monitored with GWL. Consider a geological section with three drilled boreholes as an illustration. In that situation, a central one with RP could be inserted, with both CS ends serving as a guide for the geological interpretation. Figure 15 illustrates a drilling program for

exploratory purposes in a specific and well-known geological setting, such as the Capanema Mine. About the 21 holes, 13 will be drilled with CS, 8 with RP, and all wells will have GWL. An RP borehole generates an economy for a CS borehole while costing 35% less than a CS borehole. A time consideration exists in addition to cost reduction because a CS takes much longer to complete than an RP borehole. The complexity of the geology and the level of detail needed for the project are two factors that affect all these changes.

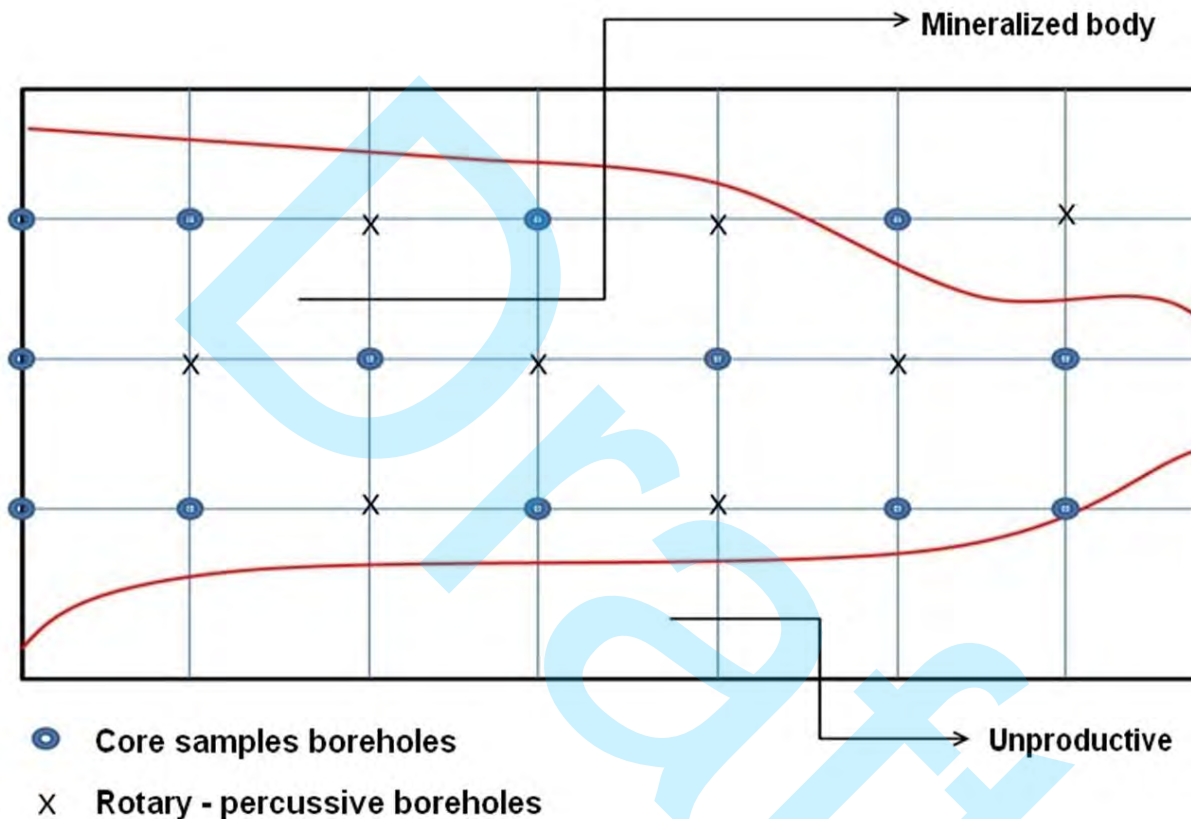


Figure 15. Programming hypothetical ore prospecting, showing the possibility of changing mesh drilling by replacing some CS with RP boreholes, using GWL to reduce time and costs in the survey (Fonseca, 2014).

CONCLUSIONS

To increase the use of geophysical well logs in mineral prospecting, the Brazilian mining company Vale S/A constructed a test site to calibrate these methods, especially the density log, whose measured property is significant for exploitation. Thus, three Capanema Mine boreholes were chosen to benefit from this initiative and advance this work. The study's primary goal was to demonstrate the value of joint interpretation of core sample data and logs in the delimitation of iron ores. The results show the importance of this method for locating the transition between friable and compact itabirites, defining lithological interfaces, detecting clay horizons, estimating the thickness of weathering layers, and identifying hydrated materials. In general, the

impact of increasing compression with depth on the density log measurements was more significant than the reduction in the content of heavy iron-rich minerals from 90 m depth during the analysis of itabirites. At this depth, the density log's value changes from 2.80 to 3.24 gr/cm³, and the sonic log's average value increases from 2000 to 7000 m/sec, indicating this fact. This study offers essential subsidies to improve methodologies applied for iron ores prospecting. It helps reduce research time and costs associated with mineral exploration when it is suggested to change the drilling mesh by substituting more rotary-percussive boreholes for core sample perforations, but always using geophysical well logs in both cases to support the geological interpretation of the subsurface.

ACKNOWLEDGEMENTS

The authors thank the Brazilian mining company Vale S/A, the Federal University of Ouro Preto (UFOP), the Brazilian National Research Agency (CNPq), the Petroleum Engineering and Exploration Laboratory (UENF/LENEP), Geoactive Limited (Interactive Petrophysics software), and National Institute of Geophysical Science and Technology (INCT-GP) for supporting this work.

REFERENCES

- Cannon, S. 2016. *Petrophysics: a practical guide*. John Wiley & Sons, Ltd, The Atrium, West Sussex, UK, 217 p.
- Darling, T. 2005. *Well, logging and formation evaluation*. Gulf Professional Publishing, Houston, TX, USA. 336 pp.
- Fonseca, L. 2000. *Mineralogical characterization of the Run of Mine of Capanema Mine*. Serra Geral Mines, Vale, Internal Report, Brazil, 20 p. (in Portuguese).
- Fonseca, L. 2014. *Evaluation of geophysical logging methods in iron ore research - case study: definition of lithologic contacts in Mina Capanema, MG*. Master's Thesis, Department of Geology, Mines School of the Federal University of Ouro Preto (UFOP), Ouro Preto, MG, Brazil, 120 p. (in Portuguese).
- Franco, A. 2003. *Geometry and tectonic evolution of the syncline Ouro Fino, Iron Quadrangle, MG*. Master's Thesis, Department of Geology, Mines School of the Federal University of Ouro Preto (UFOP), Ouro Preto, MG, Brazil, 102 p. (in Portuguese).
- Guimarães, F; Massahud, J & Viveiros, J. 1986. *Capanema iron mine in the central part of the Iron Quadrangle, Minas Gerais. Main Mineral Deposits of Brazil*. DNPM / CVRD, Brasília, DF, Brazil, Vol. II, p. 97-101 (in Portuguese).
- IPT. 2011. *Technological control of concrete with different densities is employed in executing gamma-gamma ray log calibration blocks*. Technological Research Institute, Internal Report, Vale, Brazil, 29 p. (in Portuguese).
- Kearey, P.; Brooks, M. & Hill, I. 2002. *An introduction to geophysical exploration*. 3rd ed., Blackwell Science Ltd., London, 281 p.

- Luthi, S. 2001. Geological well logs: their use in reservoir modeling. Springer - Verlag, Berlin, Heidelberg, 373 p., doi: 10.1007/978-3-662-04627-2.
- Matlab. 2014. User's Manual (<http://www.mathworks.com>).
- Pena, N. 2013. Acoustic & optical televiewer. Weatherford, Wireline Slimline Services, Internal Report, 18 p.
- Oliveira, S.; Uendro, C.; Paranhos, G.; Carmo, R. & Braga, M. 2011. Gamma-gamma ray geophysical logging as a tool to aid in the description and geological interpretation. 2nd Seminar of the Geology of Iron Ore and 1st of Speleology. VALE, Belo Horizonte, 75 p. (in Portuguese).
- Rashidi, B.; Hareland, G. & Shirkavand, F. 2009. Lithological determination from logs. Canadian International Petroleum Conference (CIPC), Calgary, Alberta, Canada. 8 p., doi: 10.2118/2009-180.
- Rider, M. 2002. The geological interpretation of well logs. Whittles Publishing, Malta, 280 p.
- Schön, J. 2011. Physical Properties of Rocks: A Workbook. Handbook of Petroleum Exploration and Production. Vol. 8. Elsevier, Amsterdam, 494 pp., doi: 10.1016/c2010-0-67039-8.
- Spier, C.; Oliveira, S.; Sial, A. & Rios, F. 2007. Geochemistry and genesis of the banded iron formations of the Caue Formation, Quadrilátero Ferrífero, Minas Gerais, Brazil. Precambrian Research, v. 152, p. 170-206, doi: 10.1016/j.precamres.2006.10.003.
- Vaz de Melo, M. & Seabra, A. 2000. Economic Geology of the Iron Ore of São Vicente Mine, Itabirito, MG. Internal Report, Serra General Mining Company, Internal Report, Brazil, 69 p. (in Portuguese).
- WellCad. 2014. WellCad User's Manual. Advanced Logic Technology, Luxembourg, 29 p.

Received on November 21, 2021 / Accepted on August 19, 2023

Carrasquilla, A.G.: proposed the work, worked on the interpretation of data, wrote the text of the article, and modified the final figures; **Fonseca, L.:** worked on the master's thesis and data modeling.